Biological Conservation 321 (2026) 111953

Contents lists available at ScienceDirect

Biological Conservation

journal homepage: www.elsevier.com/locate/biocon

Most individuals, few sites: spatial concentration of threatened butterfly populations challenges occurrence-based conservation

Markus Franzén [a,b,*], Victor Johansson [a,c]

[a] Department of Physics, Chemistry and Biology (IFM), Linköping University, SE-581 83, Linköping, Sweden
[b] Centre for Ecology and Evolution in Microbial Model Systems (EEMiS), Department of Biology and Environmental Science, Linnaeus University, SE-391 82, Kalmar, Sweden
[c] Calluna AB, Linköpings Slott, SE-582 28, Linköping, Sweden

ARTICLE INFO

Keywords:
Conservation prioritisation
Density heterogeneity
EU Habitats Directive
Gini coefficient
Lorenz curve
Spatial aggregation

ABSTRACT

Conservation planning typically relies on species occurrence records, yet where individuals concentrate within occupied landscapes may matter more for population persistence than where species are merely detected. We applied Lorenz curves and Gini coefficients, metrics originally developed to quantify wealth inequality, to spatially referenced abundance data for three threatened grassland butterflies protected under the EU Habitats Directive: *Euphydryas aurinia*, *Parnassius apollo*, and *Phengaris arion*. Across a 60 km^2 landscape on Gotland, Sweden, subdivided into 1-ha grid cells (795 species × grid observations), peak densities were strongly right-skewed and spatially concentrated for all three species. The top 19% of occupied grids accounted for 44–53% of the summed peak counts, and capturing 50% of the summed peak counts required only 20–25% of occupied grids. *Phengaris arion* was the most spatially concentrated species, and *P. apollo* the least, a ranking that was robust across Gini coefficients and concentration metrics. Habitat associations were species-specific: ground moisture and grassland proportion were positively associated with peak density for *E. aurinia* and grassland proportion for *P. apollo*, whereas *Ph. arion* peak densities declined with increasing grassland proportion and were poorly predicted by the landscape-scale habitat metrics examined. These findings demonstrate that high-density supersites can be difficult to identify from occurrence-based assessments, yet may represent important targets for population-focused conservation. The Lorenz–Gini framework provides a transferable, metric-based approach for identifying such sites across taxa, complementing area-based conservation targets by explicitly considering where populations actually persist.

1. Introduction

Animal populations are rarely distributed uniformly across landscapes. Instead, individuals aggregate spatially, and population density often varies predictably according to Taylor's power law, which relates variance to mean abundance (Taylor, 1961). This fundamental pattern, in which most occupied sites support few individuals while a minority harbour disproportionately large numbers, has profound implications for species persistence and conservation (Hanski and Gyllenberg, 1997). Source–sink dynamics further reinforce spatial heterogeneity, as productive core areas may generate demographic surpluses that sustain populations in marginal habitats (Pulliam, 1988). Extreme spatial concentration has been documented across taxa, including colonial seabirds and marine fishes (Ciannelli et al., 2013; Jovani et al., 2008; Sadovy and Domeier, 2005), suggesting that highly uneven abundance distributions may reflect general ecological processes. For threatened species experiencing range contractions, identifying high-density sites may therefore be critical, yet conservation assessments and planning often rely primarily on occurrence, occupied area, or habitat extent when spatially explicit abundance data are unavailable.

Spatially explicit abundance data are often lacking, even for well-studied taxa, yet such data are of substantial importance for assessing conservation status and setting conservation priorities, because the demographic value of a site cannot be inferred from occurrence alone. Even when abundance data are available, the way individuals are distributed across space is itself central to conservation, because abundance hotspots, the subset of sites contributing disproportionately to overall population size, may represent the most important targets for

* Corresponding author at: Department of Physics, Chemistry and Biology, Linköping University, SE-581 83, Linköping, Sweden.
E-mail address: markus.franzen@liu.se (M. Franzén).

https://doi.org/10.1016/j.biocon.2026.111953
Received 18 February 2026; Received in revised form 31 May 2026; Accepted 4 June 2026
Available online 16 June 2026

safeguarding population persistence. The mismatch between occurrence and density is likely to be especially consequential for taxa that persist as spatially structured populations in fragmented landscapes, where a few high-density patches may contribute disproportionately to metapopulation persistence. European grassland butterflies exemplify this situation. The EU Grassland Butterfly Indicator declined by 47% between 1991 and 2024 (van Swaay et al., 2026), reflecting continuing pressures from agricultural intensification, abandonment of traditional grazing, nitrogen deposition, and habitat fragmentation (WallisDeVries and van Swaay, 2006; Warren et al., 2021). Many grassland butterflies persist as metapopulations in which long-term persistence depends disproportionately on large, connected, and productive habitat patches (Hanski, 1998; Hanski and Ovaskainen, 2000; Johansson et al., 2020). Quantifying how individuals are concentrated within occupied landscapes is therefore central for identifying sites that contribute most strongly to population-level conservation value.

Species distribution models and occurrence maps typically predict where species occur but not how many individuals occur there; occurrence-based and density-based site rankings show only 10–58% overlap (Johnston et al., 2015), suggesting that area-based targets alone may be insufficient without explicit consideration of population concentration (Dinerstein et al., 2019; Kukkala and Moilanen, 2013). Lorenz curves and Gini coefficients, originally developed to quantify wealth inequality, offer a simple framework for describing such concentration. A Lorenz curve shows the cumulative proportion of individuals accounted for by the cumulative proportion of sites, ranked from lowest to highest abundance, whereas the Gini coefficient summarises the resulting inequality on a scale from 0, complete equality, to 1, extreme concentration. Weiner and Solbrig (1984) pioneered ecological applications of these indices to characterise size hierarchies in plant populations, and Gini coefficients have since been used to quantify evenness in species assemblages (Wittebolle et al., 2009) and inequality in protected area coverage (Barr et al., 2011). Many metrics can describe spatial aggregation or skewed abundance distributions, including variance-to-mean ratios, occupancy–abundance relationships, and top-site abundance shares. The advantage of Lorenz–Gini analysis is that it directly answers a conservation-relevant question: what fraction of sites contains a given fraction of individuals? Despite this interpretability, applications to spatial population structure, measuring how unevenly individuals are distributed across occupied sites, remain uncommon in conservation prioritisation, even as systematic conservation planning seeks to allocate limited resources efficiently (Margules and Pressey, 2000) and the “30 by 30” target of the Kunming–Montreal Global Biodiversity Framework underscores the urgency of identifying which sites disproportionately contribute to population persistence (Convention on Biological Diversity, 2022).

We use three threatened grassland butterflies protected under the EU Habitats Directive as a model system: the marsh fritillary (*Euphydryas aurinia*), Apollo (*Parnassius apollo*), and large blue (*Phengaris arion*). All three are habitat specialists, but they differ in habitat associations, resource requirements, and life-history constraints. *Euphydryas aurinia* is associated with wet grasslands and uses *Succisa pratensis* as its local larval host plant; *P. apollo* occurs mainly in dry, rocky habitats; and *Ph. arion* occupies relatively dry to intermediate grassland habitats where suitable *Thymus* host plants and host ants co-occur (Elmes et al., 1998; Hayes, 2015; Thomas et al., 2009; Todisco et al., 2010; Warren, 1994). Because *Ph. arion* depends on both larval host plants and host ants, its distribution may be particularly sensitive to fine-scale habitat structure. However, differences among species may also reflect dispersal capacity, resource abundance, habitat configuration, and survey-scale effects. Gotland, Sweden's largest island, provides a landscape where these ecologically contrasting species co-occur. Its calcareous grasslands and alvar habitats, maintained by harsh environmental conditions and grazing, support some of the largest remaining populations of all three species in Sweden and the Baltic region (Franzén et al., 2022, 2024b; Johansson et al., 2020).

This study quantifies spatial population concentration and identifies broad environmental correlates across a landscape subdivided into 1-ha grid cells, yielding 795 species × grid observations. We apply Lorenz–Gini analysis as a transferable framework for species with spatially referenced abundance data and use peak grid-level densities to identify supersites, defined as the highest-density 5% of grids within each species. Specifically, we test three hypotheses. H1 (spatial aggregation): peak grid-level densities are strongly right-skewed, such that a small fraction of occupied grid cells supports a disproportionately large share of summed peak counts. H2 (species differences): the degree and form of spatial concentration differ among species, reflecting differences in habitat association, resource requirements, and spatial ecology. H3 (environmental correlates): peak grid-level densities are conditionally associated with grassland proportion, ground moisture, and shrub cover; these variables provide reproducible landscape-scale predictors, while unmeasured fine-scale factors such as host-plant abundance, host-ant availability, nectar resources, and microclimate may explain additional residual spatial structure.

2. Materials and methods

2.1. Study area

Field data were collected on Gotland, Sweden's largest island (3140 km^2) in the Baltic Sea, which is characterised by a limestone-dominated landscape with semi-natural grasslands, shrublands, and open limestone pavements interspersed with coniferous forest patches and arable fields. The primary study area encompassed approximately 60 km^2 near Slite in the northeastern part of the island (57°41′ N, 18°41′ E) (Fig. 1). This landscape sustains regionally important populations of multiple threatened grassland butterflies (Franzén et al., 2022; Johansson et al., 2020). The climate is temperate, with a mean annual temperature of 7.2 °C (July mean 16.6 °C; February mean − 2.1 °C) and mean annual precipitation of 524 mm (Franzén et al., 2022). The region supports at least 15 habitat types listed under the EU Habitats Directive.

2.2. Study species

We focused on three butterfly species listed under the EU Habitats Directive that co-occur in this landscape: *Euphydryas aurinia* (Rottemburg, 1775) (marsh fritillary; Annex II), *Parnassius apollo* (Linnaeus, 1758) (Apollo; Annex IV), and *Phengaris* (formerly *Maculinea*) *arion* (Linnaeus, 1758) (large blue; Annex IV). All three are nationally Red-listed in Sweden yet retain large populations on Gotland (Franzén et al., 2022). These species are habitat specialists associated with open grassland, but differ in their ecological requirements: *E. aurinia* occupies damp grasslands with its sole local larval host plant, *Succisa pratensis*; *P. apollo* inhabits dry, rocky grasslands with *Sedum* species as larval hosts; and *Ph. arion* requires short-sward grasslands supporting both its larval host plant, *Thymus serpyllum*, and colonies of its obligate host ant, *Myrmica sabuleti* (Elmes et al., 1998; Hayes, 2015; Thomas et al., 2009). We analysed data from a single focal year per species, selected as the year with the most comprehensive spatial coverage: *E. aurinia*, 2017; *P. apollo*, 2019; *Ph. arion*, 2025. These focal years derive from independent, intensive monitoring projects conducted in the same landscape and represent the only years with near-complete spatial coverage and sufficiently high survey effort and butterfly counts to permit robust quantification of spatial population concentration at 1-ha resolution.

2.3. Survey design and data filtering

We conducted a systematic landscape-scale survey in which all suitable open habitat within the 60 km^2 study area was mapped and subdivided into a contiguous grid of 100 × 100 m cells, each representing 1 ha and producing hundreds of spatial sampling units. One-hectare grids provide a practical and repeatable survey unit that a

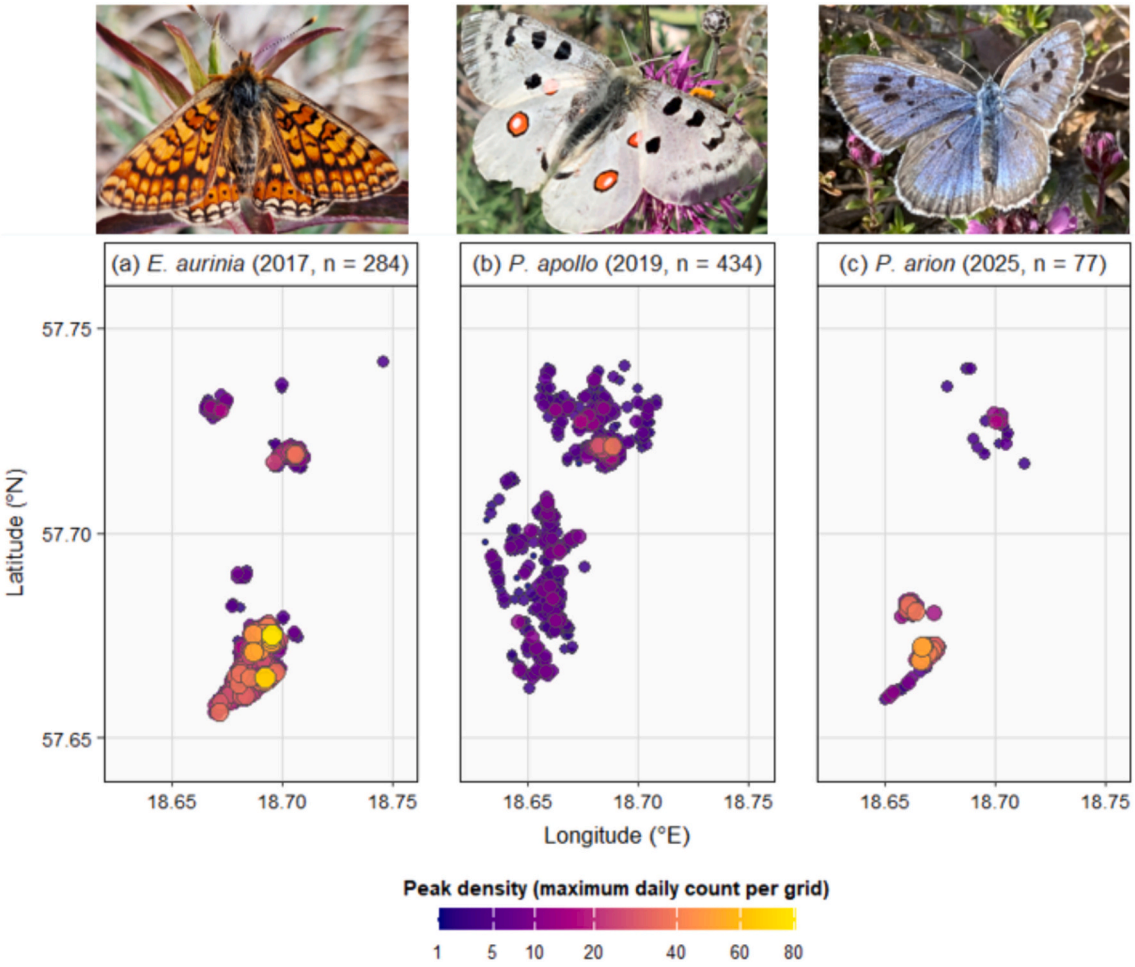

Fig. 1. Spatial distribution and peak densities of three threatened butterfly species on Gotland, Sweden, with representative photographs of each species. Points represent occupied 1 ha grid cells surveyed on at least three distinct dates during the focal year: (a) *Euphydryas aurinia* (2017, n = 284), (b) *Parnassius apollo* (2019, n = 434), and (c) *Phengaris arion* (2025, n = 77). Point size and colour are scaled to peak density, defined as the maximum daily adult count per grid, according to the shared colour ramp shown below the panels. Note differing spatial extents of occupied grids among species.

single observer can thoroughly search during one visit. This resolution is also comparable to the median lifetime net-displacement distances reported for the focal species, defined as the straight-line distance between first and last capture locations for each individual: 0.135 km for *E. aurinia*, 0.253 km for *P. apollo*, and 0.252 km for *Ph. arion* (Franzén et al., 2025). The grid scale was therefore appropriate for capturing fine-scale density variation among sites. Observers conducted zigzag searches across each grid cell during favourable weather conditions ($\geq$17 °C, wind <8 m s^{-1}, no rain, 08:00–18:00 h) and recorded the number of adult individuals observed. Grid cells were surveyed repeatedly throughout the flight season of each focal species. A visit was defined as a single survey of a given grid cell on a distinct day.

Rather than modelling survey effort as a covariate, we controlled for detection reliability through a design-based effort filter: only occupied grid cells surveyed on at least three distinct dates during the focal season were retained. For each retained grid cell, we defined peak density as the maximum single-day adult count observed within the focal year. This yielded one record per species per grid cell, with peak count as the response variable. Because the retained analytical dataset consisted of occupied grids with positive peak counts, all response values were ≥ 1, a property accounted for by the zero-truncated models described below. After filtering, the dataset comprised 795 species × grid observations: 284 grids for *E. aurinia*, 434 for *P. apollo*, and 77 for *Ph. arion*.

2.4. Habitat predictors

We quantified habitat structure and surface moisture using the Swedish National Land Cover Dataset (Nationella Marktäckedata, NMD 2018; Swedish Environmental Protection Agency, 2020), produced from satellite imagery and airborne LiDAR data. All habitat variables were aggregated to the 1-ha grid level, using mean values across the 100 underlying 10 × 10 m pixels within each grid cell; no point-exact or visit-level environmental data were used. For each grid cell, we extracted three habitat variables: (1) grassland proportion, defined as the proportion of the grid cell classified as open grassland habitat; (2) ground moisture index (GMI), derived from the Markfuktighetsindex of the Swedish National Land Cover Dataset (Swedish Environmental Protection Agency, 2022), which combines depth-to-water estimates with a soil topographic wetness index, where higher values indicate wetter, more mesic conditions; and (3) shrub cover, defined as the percentage of the grid cell covered by shrubs or woody vegetation (0.5–5 m height as classified by the NMD), indicative of successional encroachment.

Pairwise correlations among habitat predictors were weak to moderate across species (Pearson $|r| = 0.10$–0.38; $n = 77$–434 grids per species). No predictor pair exceeded $|r| = 0.7$ for any species, indicating that collinearity did not warrant predictor exclusion (Dormann et al., 2013). Grassland proportion and shrub cover showed no consistent directional relationship across species (Pearson $r = -0.22$ to 0.16),

whereas ground moisture and shrub cover were moderately negatively correlated in the two larger datasets ($r = -0.38$ to -0.37; $n = 284$–434). Habitat effects are therefore interpreted as conditional associations. Full per-species correlation matrices are provided in Table S4. All continuous habitat predictors were z-standardised (mean = 0, SD = 1) prior to analysis to facilitate comparison of effect sizes and ensure model convergence.

2.5. Statistical analysis

All analyses were conducted in R version 4.5.1 (R Core Team, 2025). We addressed the three hypotheses sequentially: spatial concentration (H1) was quantified using Lorenz–Gini analysis; cross-species differences in concentration (H2) were assessed by comparing species-specific Gini coefficients and concentration metrics; and environmental correlates of density (H3) were modelled using species-specific regression models.

2.5.1. Spatial concentration (H1, H2)

For each species, we ranked grid cells by peak density and constructed Lorenz curves plotting the cumulative proportion of total observed peak counts against the cumulative proportion of grid cells, ordered from lowest to highest peak density. We calculated the Gini coefficient (G) using the standard formula (Damgaard and Weiner, 2000; Weiner and Solbrig, 1984), where G ranges from 0 (uniform distribution) to 1 (maximum concentration). We additionally quantified the minimum proportion of grid cells required to contain 50%, 80%, and 90% of the total observed peak counts for each species. To test whether spatial concentration differed among species (H2), we computed 95% bias-corrected and accelerated (BCa) bootstrap confidence intervals for each species-specific Gini coefficient (10,000 resamples) and tested pairwise differences using permutation tests (10,000 permutations).

2.5.2. Environmental correlates of peak density (H3)

We modelled peak density (maximum single-day count) using zero-truncated negative binomial (ZTNB) regression (NB2 parameterisation, log link; glmmTMB package; Brooks et al., 2017). Zero truncation was appropriate because peak density was defined only for grid cells with retained occupied grids and therefore strictly positive counts (Zuur et al., 2009). For each species, the response variable was the peak adult count per grid cell, with grassland proportion, GMI, and shrub cover (all z-standardised) as fixed-effect predictors. We fitted separate models for each species because the three species differ fundamentally in their habitat requirements (Section 2.2); a pooled model would obscure species-specific associations that are central to H3.

Model assumptions were evaluated using simulated residual diagnostics (DHARMa package; Hartig, 2022). Coefficients are reported as incidence rate ratios (IRR = exp(β)) with Wald-based 95% confidence intervals, representing the multiplicative change in expected peak count per one standard deviation increase in the predictor.

2.5.3. Spatial autocorrelation

Residual spatial autocorrelation was assessed using Moran's I computed on Pearson residuals from the ZTNB models (spdep package; Bivand et al., 2013). Spatial neighbours were defined using a distance threshold of 1000 m, with row-standardised weights. Significance was assessed using the normal approximation.

2.5.4. Sensitivity analyses

To evaluate potential residual spatial structure beyond the measured habitat predictors, we fitted generalised additive models (GAMs) including a two-dimensional thin-plate regression spline of grid coordinates, implemented using mgcv::bam() with fast REML estimation (Wood, 2017). The basis dimension (k) was set to min(60, ⌊n/2⌋) per species, yielding k = 38 for *Ph. arion* ($n = 77$) and k = 60 for the two larger datasets. These GAMs used a standard (non-truncated) negative binomial family and were interpreted qualitatively as a diagnostic for unmeasured spatial structure; because they use a different likelihood from the main models, coefficients are compared for effect direction only, not magnitude.

2.5.5. Multiple testing

We fitted separate ZTNB models per species, each including three habitat predictors, yielding nine individual coefficient tests. Species-specific models were biologically motivated: the three species differ in spatial extent, occupy distinct ecological niches, and were surveyed in different focal years; a pooled model would obscure these differences. We report uncorrected *p*-values throughout and interpret individual coefficients cautiously, emphasising effect sizes, confidence intervals, and the consistency of effect directions across species rather than relying on significance thresholds alone. All four originally significant associations remained significant after Holm correction for the nine tests (Holm, 1979).

3. Results

3.1. Spatial concentration and interspecific variation (H1, H2)

Peak butterfly densities were right-skewed and spatially concentrated across the landscape for all three species (Table 1; Fig. 2a). Coefficients of variation in peak density ranged from 0.82 to 0.95. *Euphydryas aurinia* attained the highest within-grid peak densities (maximum 81 individuals ha^{-1}; mean 15.1, median 12; $n = 284$ grids), followed by *Ph. arion* (maximum 53; mean 13.9, median 10; $n = 77$) and *P. apollo* (maximum 38; mean 4.7, median 4; $n = 434$; Table 1). Mapped distributions revealed distinct spatial hotspots of high density within the study area (Fig. 1).

Lorenz curves and Gini coefficients confirmed that peak densities were spatially concentrated for all species (H1) and revealed interspecific differences in the degree of concentration (H2; Fig. 2; Table S1). *Phengaris arion* was the most spatially concentrated (Gini = 0.50, 95% BCa CI 0.45–0.55), followed by *E. aurinia* (0.42, 0.39–0.45) and *P. apollo* (0.37, 0.34–0.40); pairwise permutation tests confirmed that all three species differed significantly in spatial concentration (all $p \leq 0.015$), supporting H2. The proportion of grids required to capture 50%, 80%, and 90% of summed peak counts further illustrated this concentration (Fig. S1; Table S1). The top 19% of occupied grids contained 53% of all *Ph. arion* summed peak counts, compared with 46% for *E. aurinia* and 44% for *P. apollo*. Conversely, capturing 50% of summed peak counts required only 19% of grids for *Ph. arion* (15 of 77), versus 23% for *E. aurinia* and 25% for *P. apollo*. The species ranking was consistent across the Gini coefficient, the share of individuals in the top 10% and top 19% of grids, and the proportion of grids required to capture 50%, 80%, or 90% of summed peak counts: *Ph. arion* was the most concentrated species and *P. apollo* the least across all integrated metrics.

Supersites were defined as grids with peak densities at or above the 95th percentile within each species and accounted for a disproportionate share of summed peak counts (Table S1). The single highest-density grid contributed 4.9% of total *Ph. arion* summed peak counts, compared with 1.9% for both *E. aurinia* and *P. apollo*. Expressed relative to an equal distribution across occupied grids, the highest-density grid represented 3.8 times the expected share for *Ph. arion*, compared with 5.4 times for *E. aurinia* and 8.0 times for *P. apollo*. This single-cell ratio gives a different ranking from the integrated metrics above, because the ratio scales linearly with the number of occupied grids and is therefore dominated by sample size rather than by the depth of concentration in the tail of the abundance distribution. The integrated metrics, which characterise the full distribution of peak counts across occupied grids, all converge on the same species ranking.

Table 1
Sample characteristics and peak density distributions for three threatened butterfly species on Gotland, Sweden. Peak density is defined as the maximum daily adult count per 1 ha grid cell. Only occupied grids surveyed on at least three distinct dates during the focal year were included. CV = coefficient of variation.

Species	Year	n grids	Total peak counts	Median	Mean (SD)	Range	CV
Euphydryas aurinia	2017	284	4279	12	15.07 (12.31)	1–81	0.82
Parnassius apollo	2019	434	2050	4	4.72 (3.93)	1–38	0.83
Phengaris arion	2025	77	1072	10	13.92 (13.25)	1–53	0.95

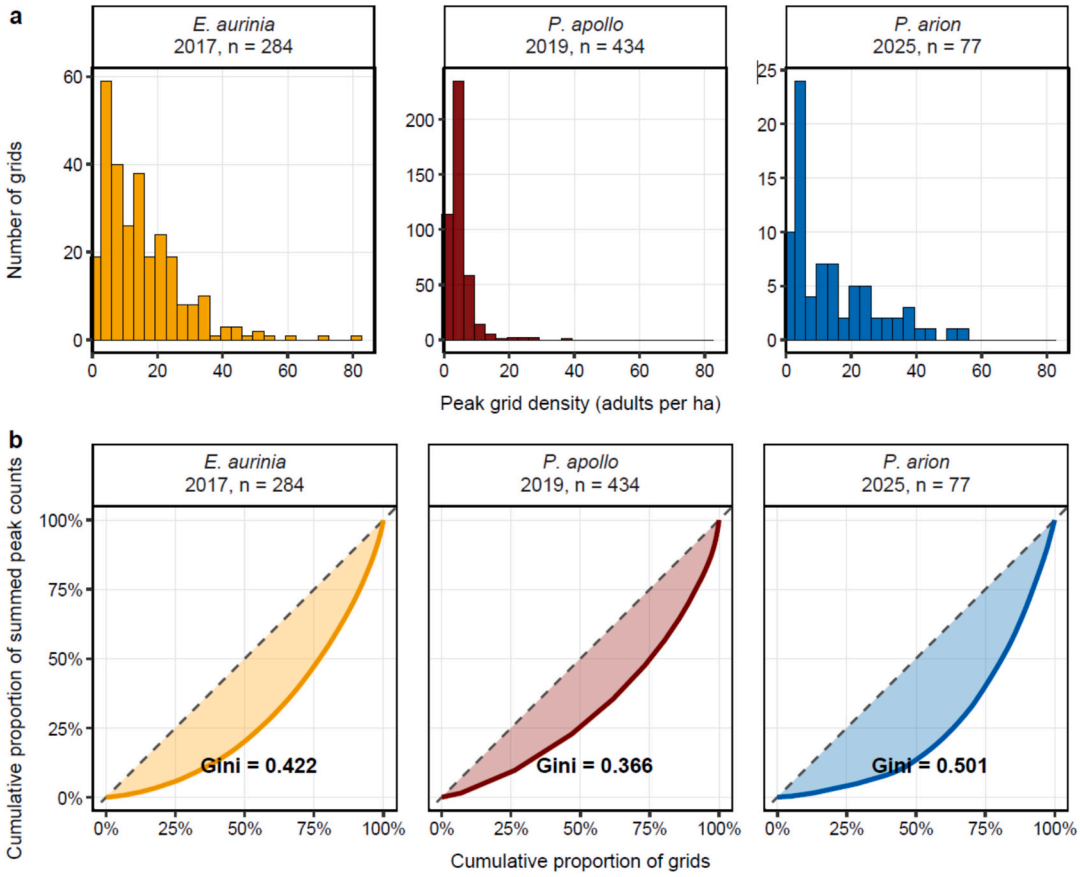

Fig. 2. Frequency distributions and Lorenz curves showing the spatial concentration of peak butterfly densities across 1-ha grid cells on Gotland, Sweden. Histograms (a) show the frequency distribution of peak grid densities, defined as the maximum daily adult count per 1-ha grid. Note that the histogram y-axis scales differ among species. Lorenz curves (b) show the cumulative proportion of grids ranked from lowest to highest density on the x-axis and the cumulative proportion of summed peak counts on the y-axis. The diagonal line represents perfect equality, where all grids contribute equally to the summed peak counts. The shaded area between each curve and the diagonal is proportional to the Gini coefficient, shown within each panel. Histograms visualise skewed peak-density distributions, whereas Lorenz curves and Gini coefficients quantify cumulative concentration across all occupied grids.

Table 2
Environmental predictors of peak density for three threatened butterfly species on Gotland, Sweden. Incidence rate ratios (IRR) from species-specific zero-truncated negative binomial models of peak density. All continuous predictors are z-standardised; effects correspond to one standard deviation change. Significant effects ($p < 0.05$) are shown in bold.

Species	Predictor	IRR	95% CI	p
E. aurinia	Grassland	1.19	1.08–1.32	< 0.001
	GMI	1.34	1.21–1.49	< 0.001
	Shrub cover	1.03	0.92–1.15	0.58
P. apollo	Grassland	1.22	1.13–1.32	< 0.001
	GMI	1.05	0.97–1.14	0.24
	Shrub cover	1.01	0.93–1.10	0.86
Ph. arion	Grassland	0.64	0.51–0.81	< 0.001
	GMI	0.99	0.77–1.28	0.95
	Shrub cover	0.88	0.71–1.10	0.27

3.2. Habitat correlates of peak density (H3)

Habitat associations with peak density differed among species (Table 2; Fig. 3). In species-specific zero-truncated negative binomial models, *E. aurinia* peak densities increased with ground moisture (IRR = 1.34, 95% CI 1.21–1.49, Wald z = 5.76, $p < 0.001$; $n = 284$) and grassland proportion (IRR = 1.19, 95% CI 1.08–1.32, z = 3.57, p < 0.001), whereas shrub cover showed no detectable association (IRR = 1.03, 95% CI 0.92–1.15, $p = 0.58$). *Parnassius apollo* peak densities increased with grassland proportion (IRR = 1.22, 95% CI 1.13–1.32, z = 4.95, p < 0.001; $n = 434$), with no significant associations for ground moisture ($p = 0.24$) or shrub cover ($p = 0.86$).

Ph. arion showed a contrasting pattern: peak density decreased with increasing grassland proportion (IRR = 0.64, 95% CI 0.51–0.81, z = −3.71, p < 0.001; $n = 77$), while ground moisture ($p = 0.95$) and shrub cover ($p = 0.27$) showed no significant associations. Grids embedded in more extensive grassland landscapes did not correspond to higher peak densities for this species.

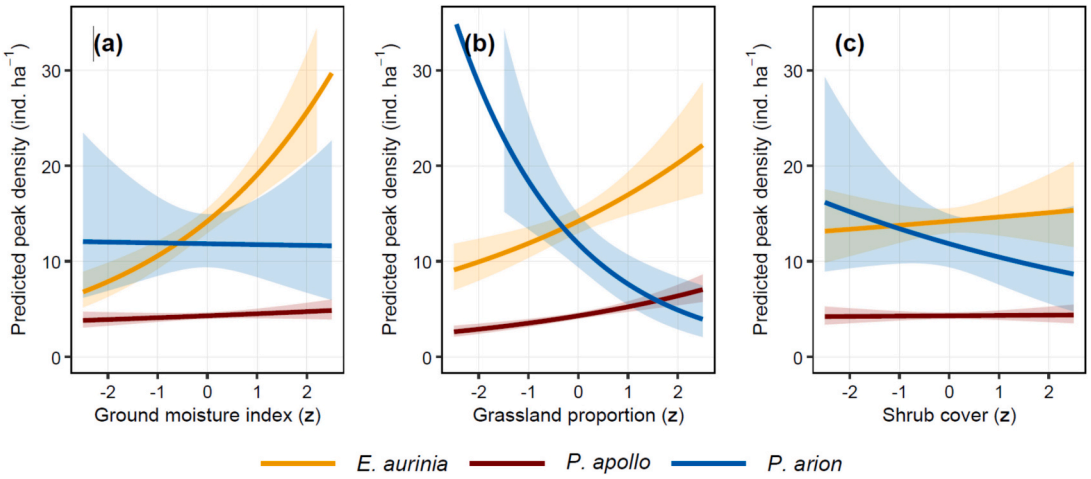

Fig. 3. Predicted peak density as a function of three habitat predictors for three threatened butterfly species on Gotland, Sweden: (a) ground moisture index, (b) grassland proportion, and (c) shrub cover. Lines show predicted values from species-specific zero-truncated negative binomial models; shaded bands represent 95% confidence intervals. Each predictor is z-standardised; predictions are computed with remaining predictors held at their mean values. See Table 2 for model coefficients.

Moran's I tests on Pearson residuals from the ZTNB models detected significant positive residual spatial autocorrelation for all three species (*E. aurinia*: $I = 0.11$, $p < 0.001$; *P. apollo*: $I = 0.10$, $p < 0.001$; *Ph. arion*: $I = 0.15$, $p < 0.001$; Table S2), indicating spatial structure in peak densities not fully captured by the three measured habitat predictors. GAM sensitivity analyses, including a two-dimensional spatial smooth, confirmed significant residual spatial structure for all species (*E. aurinia*: edf = 32.7, $p < 0.001$; *P. apollo*: edf = 33.0, $p < 0.001$; *Ph. arion*: edf = 6.0, $p = 0.002$; Table S3), suggesting that unmeasured spatially structured factors influence peak densities beyond the habitat variables considered here. Habitat predictor effect directions were consistent between the main ZTNB models and the GAMs for eight of nine species–predictor combinations (Table 2; Table S3); the exception was shrub cover for *P. apollo*, which was non-significant in the ZTNB model but significantly negative in the GAM. These results partially support H3: habitat variables explained variation in peak densities most strongly for *E. aurinia*, for which two of three predictors were significant; *P. apollo* was associated with grassland proportion only; and *Ph. arion* peak densities declined with grassland proportion but were otherwise not well predicted by the landscape-scale habitat metrics examined (Table 2; Fig. 3).

4. Discussion

Conservation planning typically relies on species occurrence records, yet where individuals concentrate within occupied landscapes may matter more for population persistence than where they are merely detected. Our results confirm that peak densities of three ecologically contrasting butterfly species were spatially concentrated rather than uniformly distributed across the landscape (H1). The degree of concentration differed among species, with *Ph. arion* most concentrated, followed by *E. aurinia* and *P. apollo* (H2). This ranking was robust across multiple concentration metrics, including the Gini coefficient, the share of individuals in the top 10% and top 19% of grids, and the proportion of grids required to capture 50%, 80%, or 90% of individuals. Environmental correlates of peak density were nevertheless species-specific and only partially explained by the landscape-scale habitat metrics we examined (H3), particularly for *P. apollo* and *Ph. arion*. Taken together, these findings indicate that a Lorenz–Gini framework applied to spatially referenced abundance data can reveal supersites that would be difficult to identify from occurrence-based assessments alone, but that the habitat features associated with such sites cannot be assumed to generalise across species, even within the same landscape.

4.1. Spatial concentration and interspecific variation (H1, H2)

The spatial aggregation observed across all three species is consistent with Taylor's power law, which predicts an increase in variance with mean abundance in ecological populations (Taylor, 1961). Lorenz–Gini analysis quantified this inequality explicitly, confirming that most grid cells supported few individuals, whereas a minority harboured disproportionately high densities. Such concentration patterns appear widespread across animal taxa. In colonial seabirds, colony size distributions are extremely right-skewed, with a small fraction of colonies supporting the majority of breeding individuals (Jovani et al., 2008). In marine fishes, spatial concentration of biomass at a minority of survey stations is sufficiently general that Lorenz-curve-derived indicators, mathematically equivalent to the Gini coefficient used here, have become standard monitoring tools (Petitgas, 1998; Woillez et al., 2007). Comparable patterns have been documented in reef fish spawning aggregations, where reproductive effort concentrates at predictable habitat features (Sadovy and Domeier, 2005; Ciannelli et al., 2013); in pond-breeding amphibians, where a minority of water bodies support the majority of breeding activity (Heard et al., 2012); and in pinnipeds, where a small number of rookeries account for most pup production (Condit et al., 2022). Recent work on the large blue butterfly *Ph. arion* reported approximately 100-fold variation in carrying capacity among restored conservation grasslands, illustrating how strongly densities can concentrate among sites even within a single species (Thomas et al., 2025). Macroecological theory predicts such concentration as a general consequence of the positive abundance–occupancy relationship: because individuals aggregate in space, a disproportionate fraction of any population will occupy a small fraction of its range (Gaston et al., 2000). The concentration patterns we document in butterflies are consistent with this prediction and suggest that Lorenz–Gini analysis offers a transferable framework for quantifying spatial inequality across taxa.

Spatial concentration differed among species in a pattern that was robust to the choice of concentration metric. *Phengaris arion* showed the highest Gini coefficient (0.50), the highest share of individuals in the top 10% and top 19% of grids (32% and 53% respectively), and the lowest proportion of grids required to capture 50%, 80%, or 90% of the population (19%, 43%, and 56% respectively). *Parnassius apollo* showed the lowest values on the same metrics, and *E. aurinia* fell consistently between the two. An alternative descriptor, the share of individuals in the single highest-density grid expressed relative to an equal distribution across occupied grids, gives the opposite ranking (*P. apollo* 8.0×,

E. aurinia 5.4×, *Ph. arion* 3.8×), because this ratio scales linearly with the number of occupied grids and is therefore dominated by sample size rather than by the depth of concentration in the tail of the abundance distribution. The Gini-based ranking is consistent with theory predicting that species with narrower ecological niches should exhibit stronger spatial concentration, because suitable conditions occur in a more limited subset of sites (Brown, 1984; Slatyer et al., 2013). However, the species comparison rests on three taxa, and differences in dispersal capacity, wing size, host-resource distribution, habitat configuration, and local management history may also influence how individuals are distributed among occupied grids. Data from additional species would be needed to test whether ecological specialisation predicts spatial concentration more generally.

4.2. Habitat correlates and the predictability of supersites (H3)

Species-specific habitat associations provide partial insight into the mechanisms underlying spatial concentration. For *E. aurinia*, positive associations with ground moisture and grassland proportion are consistent with its dependence on damp grasslands supporting its host plant *Succisa pratensis* (Warren, 1994; Schtickzelle et al., 2005). *Parnassius apollo* showed weaker and more diffuse associations, suggesting that factors beyond the three landscape-scale predictors examined here, such as host plant availability, microclimate, or topographic exposure, may influence local densities (Todisco et al., 2010). *Phengaris arion* peak densities declined with increasing grassland proportion, indicating that visually extensive grasslands do not necessarily correspond to high local densities for this species. This negative association should not be interpreted as grassland avoidance. Instead, it probably reflects the coarse scale of the grassland metric relative to the fine-scale requirements of *Ph. arion*, which depends on the local coincidence of short-sward vegetation, larval host plants, and suitable *Myrmica* host-ant colonies (Elmes et al., 1998; Thomas et al., 2009). Extensive grassland may include large areas that are structurally unsuitable if they lack warm, short, and heterogeneous microhabitats. In this landscape, the negative association may also partly reflect post-drought spatial dynamics, because *Ph. arion* used areas with more tree cover during the 2018 drought, and some open grassland grids that were occupied before 2018 have not yet been fully recolonised, contributing low or zero peak counts to the grassland end of the gradient. Similar scale mismatches appear common in European *Phengaris* butterflies: *Phengaris* butterflies can concentrate near natural patch edges, probably because such edges influence host-ant distributions (Nowicki et al., 2013), and large alluvial meadows may fail to provide suitable host-ant habitat for *Ph. nausithous* despite appearing broadly suitable as grassland (Pech et al., 2026). Broad grassland cover alone is therefore a poor proxy for high-quality *Ph. arion* habitat.

Despite including key habitat predictors, significant residual spatial autocorrelation remained for all species (Table S2), and GAM sensitivity analyses confirmed spatial structure beyond the measured habitat variables (Table S3). Such residual structure is commonly reported in spatial abundance models and may reflect unmeasured spatially varying factors, such as fine-scale host plant density, microclimate, or historical land use (Fretwell and Lucas, 1969; Hanski, 1998; Hanski and Ovaskainen, 2000). Dispersal processes may also contribute: movement among habitat patches in these species is shaped by landscape properties and local density (Franzén et al., 2024a), and immigration from nearby high-density grids can elevate local counts (Brown and Kodric-Brown, 1977; Hanski, 1999). Spatial concentration should therefore be interpreted as an emergent property of multiple interacting processes rather than as a consequence of any single environmental factor.

4.3. Supersites and conservation prioritisation

Taken together, these findings highlight the added value of considering spatial variation in abundance in conservation assessment and planning. Our results reinforce concerns that occurrence-based conservation tools may overlook sites of disproportionate demographic importance when abundance data are available. Species distribution models and occupancy-based prioritisation frameworks identify where species occur but do not quantify how individuals distribute among occupied sites (Kukkala and Moilanen, 2013; Margules and Pressey, 2000). Empirical comparisons show limited overlap between sites prioritised by occurrence versus abundance, implying that treating all occupied habitat as equally valuable can conflate demographic strongholds with marginal or transient populations (Johnston et al., 2015). Density-based metrics explicitly identify sites contributing disproportionately to population size. In our system, a small fraction of occupied grids accounted for a large share of the summed peak counts across all three species, illustrating how abundance-informed prioritisation can complement occurrence-based approaches. At the same time, our results caution against assuming that supersites are uniformly predictable from coarse habitat data: for *Ph. arion*, peak densities were not well predicted by the landscape-scale habitat metrics examined, underscoring the need for species-specific field assessment alongside landscape-scale modelling.

4.4. Temporal considerations

Peak densities were derived from single focal years, and spatial patterns may shift over time due to environmental fluctuations or population dynamics (Kéry and Royle, 2016; McLaughlin et al., 2002). Nevertheless, the spatial aggregation observed and its partial association with environmental gradients suggest that concentration patterns are not purely stochastic. Habitat predictors served as coarse landscape-scale proxies; incorporating finer-scale variables, such as host plant abundance, nectar resources, or ant nest density, would likely improve explanatory power, particularly for *Ph. arion*. Beyond these caveats, the temporal stability of abundance hotspots themselves remains poorly characterised, and dedicated multi-year studies are needed to determine the extent to which high-density sites persist across years or shift in response to climatic variability, management, and population dynamics.

4.5. Implications and conclusions

Our findings have direct implications for area-based conservation targets such as the Kunming–Montreal “30 by 30” framework (Convention on Biological Diversity, 2022). While protecting a large proportion of land is necessary, conservation efficiency depends on which sites are prioritised. Spatial concentration may create vulnerability: the loss of a single high-density site can disproportionately reduce regional population size, a pattern well established in metapopulation theory (Hanski, 1998; Hanski and Ovaskainen, 2000). Furthermore, habitat restoration rarely achieves a one-to-one replacement of conservation value, as restored sites are unlikely to replicate the specific conditions that sustain high local abundances (Curran et al., 2014; Maron et al., 2012). Loss avoidance at confirmed supersites should therefore take precedence over offsetting strategies. Effective conservation requires protecting networks of high-density sites rather than isolated strongholds and tailoring management to species-specific ecological contexts.

More broadly, our results illustrate that Lorenz–Gini analysis provides a readily transferable framework for quantifying spatial concentration in threatened populations. By linking abundance distributions explicitly to space, this approach complements occurrence-based methods and can identify cryptic supersites, sites of disproportionate demographic importance that would be overlooked by presence–absence assessments alone. Applying density-based spatial metrics across taxa and landscapes will be critical to ensuring that area-based conservation targets protect not only where species occur, but also those core sites contributing disproportionately to population

persistence.

CRediT authorship contribution statement

Markus Franzén: Writing – review & editing, Writing – original draft, Visualization, Validation, Supervision, Resources, Project administration, Methodology, Investigation, Funding acquisition, Formal analysis, Data curation, Conceptualization. **Victor Johansson:** Writing – review & editing, Writing – original draft, Validation, Methodology, Investigation, Funding acquisition, Formal analysis, Conceptualization.

Declaration of Generative AI and AI-assisted technologies in the writing process

During the preparation of this work the authors used Gemini (Google) for proofreading and language editing.

Funding

This work was supported by Formas (grant to M.F. and V.J., Dnr 2018-02846); the Swedish National Research Programme on Climate (grant to M.F. and V.J., Dnr 2021-02142); Stiftelsen Oscar och Lili Lamms Minne (grant to V.J., Dnr FO2020-0023); and the Carl Trygger Foundation (grant to M.F.).

Declaration of competing interest

The authors declare no competing interests.

Acknowledgements

We thank all data collectors for their invaluable assistance during field surveys. We are grateful to the County Administrative Board of Gotland for providing permits and to local farmers and landowners for access to their land.

Appendix A. Supplementary data

Supplementary data to this article can be found online at https://doi.org/10.1016/j.biocon.2026.111953.

Data availability

Data and code associated with this study are deposited in Figshare (https://doi.org/10.6084/m9.figshare.30884825).

References

Barr, L.M., Pressey, R.L., Fuller, R.A., Segan, D.B., McDonald-Madden, E., Possingham, H. P., 2011. A new way to measure the world's protected area coverage. PLoS One 6, e24707. https://doi.org/10.1371/journal.pone.0024707.

Bivand, R.S., Pebesma, E., Gómez-Rubio, V., 2013. Applied Spatial Data Analysis with R, second ed. Springer, New York.

Brooks, M.E., Kristensen, K., van Benthem, K.J., Magnusson, A., Berg, C.W., Nielsen, A., Skaug, H.J., Mächler, M., Bolker, B.M., 2017. glmmTMB balances speed and flexibility among packages for zero-inflated generalized linear mixed modeling. R J. 9, 378–400. https://doi.org/10.32614/RJ-2017-066.

Brown, J.H., 1984. On the relationship between abundance and distribution of species. Am. Nat. 124, 255–279.

Brown, J.H., Kodric-Brown, A., 1977. Turnover rates in insular biogeography: effect of immigration on extinction. Ecology 58, 445–449.

Ciannelli, L., Fisher, J.A.D., Skern-Mauritzen, M., Hunsicker, M.E., Hidalgo, M., Frank, K. T., Bailey, K.M., 2013. Theory, consequences and evidence of eroding population spatial structure in harvested marine fishes: a review. Mar. Ecol. Prog. Ser. 480, 227–243. https://doi.org/10.3354/meps10067.

Condit, R., Allen, S.G., Costa, D.P., Codde, S., Goley, P.D., Le Boeuf, B.J., Lowry, M.S., Morris, P.A., 2022. Estimating population size when individuals are asynchronous: a model illustrated with northern elephant seal breeding colonies. PLoS One 17, e0262214. https://doi.org/10.1371/journal.pone.0262214.

Convention on Biological Diversity, 2022. Kunming-Montreal Global Biodiversity Framework. CBD/COP/DEC/15/4. Secretariat of the Convention on Biological Diversity, Montreal.

Curran, M., Hellweg, S., Beck, J., 2014. Is there any empirical support for biodiversity offset policy? Ecol. Appl. 24, 617–632. https://doi.org/10.1890/13-0243.1.

Damgaard, C., Weiner, J., 2000. Describing inequality in plant size or fecundity. Ecology 81, 1139–1142. https://doi.org/10.1890/0012-9658(2000)081[1139:DIIPSO]2.0.CO;2.

Dinerstein, E., Vynne, C., Sala, E., Joshi, A.R., Fernando, S., Lovejoy, T.E., Mayorga, J., Olson, D., Asner, G.P., Baillie, J.E.M., Burgess, N.D., Burkart, K., Noss, R.F., Zhang, Y.P., Baccini, A., Birch, T., Hahn, N., Joppa, L.N., Wikramanayake, E., 2019. A global deal for nature: guiding principles, milestones, and targets. Sci. Adv. 5, eaaw2869. https://doi.org/10.1126/sciadv.aaw2869.

Dormann, C.F., Elith, J., Bacher, S., Buchmann, C., Carl, G., Carré, G., Marquéz, J.R.G., Gruber, B., Lafourcade, B., Leitão, P.J., Münkemüller, T., McClean, C., Osborne, P.E., Reineking, B., Schröder, B., Skidmore, A.K., Zurell, D., Lautenbach, S., 2013. Collinearity: a review of methods to deal with it and a simulation study evaluating their performance. Ecography 36, 27–46. https://doi.org/10.1111/j.1600-0587.2012.07348.x.

Elmes, G.W., Thomas, J.A., Wardlaw, J.C., Hochberg, M.E., Clarke, R.T., Simcox, D.J., 1998. The ecology of Myrmica ants in relation to the conservation of Maculinea butterflies. J. Insect Conserv. 2, 67–78.

Franzén, M., Francioli, Y., Askling, J., Kindvall, O., Johansson, V., Forsman, A., 2022. Differences in phenology, daily timing of activity, and associations of temperature utilization with survival in three threatened butterflies. Sci. Rep. 12, 7534. https://doi.org/10.1038/s41598-022-10676-0.

Franzén, M., Askling, J., Kindvall, O., Johansson, V., Sunde, J., Forsman, A., 2024a. Landscape properties and density dependence shape the movement patterns of three threatened butterflies. Landsc. Ecol. 39, 160. https://doi.org/10.1007/s10980-024-01963-4.

Franzén, M., Johansson, H., Askling, J., Kindvall, O., Johansson, V., Forsman, A., Sunde, J., 2024b. Long-distance movements, large population sizes and density-dependent dispersal in three threatened butterfly species. Insect Conserv. Divers. 17, 1033–1045. https://doi.org/10.1111/icad.12766.

Franzén, M., Forsman, A., Kindvall, O., Johansson, V., 2025. Distance of movement in three threatened butterfly species. Ecol. Entomol. 50, 1–11. https://doi.org/10.1111/een.70027.

Fretwell, S.D., Lucas, H.L., 1969. On territorial behavior and other factors influencing habitat distribution in birds. Acta Biotheor. 19, 16–36.

Gaston, K.J., Blackburn, T.M., Greenwood, J.J.D., Gregory, R.D., Quinn, R.M., Lawton, J. H., 2000. Abundance–occupancy relationships. J. Appl. Ecol. 37 (s1), 39–59. https://doi.org/10.1046/j.1365-2664.2000.00485.x.

Hanski, I., 1998. Metapopulation dynamics. Nature 396, 41–49.

Hanski, I., 1999. Metapopulation Ecology. Oxford University Press, Oxford.

Hanski, I., Gyllenberg, M., 1997. Uniting two general patterns in the distribution of species. Science 275, 397–400.

Hanski, I., Ovaskainen, O., 2000. The metapopulation capacity of a fragmented landscape. Nature 404, 755–758. https://doi.org/10.1038/35008063.

Hartig, F., 2022. DHARMa: Residual Diagnostics for Hierarchical (Multi-Level/Mixed) Regression Models. R Package Version 0.4.6. https://CRAN.R-project.org/package=DHARMa. (Accessed 15 November 2024).

Hayes, M.P., 2015. The biology and ecology of the large blue butterfly *Phengaris* (*Maculinea*) *arion*: a review. J. Insect Conserv. 19, 1037–1051. https://doi.org/10.1007/s10841-015-9820-3.

Heard, G.W., Scroggie, M.P., Malone, B.S., 2012. Classical metapopulation theory as a useful paradigm for the conservation of an endangered amphibian. Biol. Conserv. 148, 156–166. https://doi.org/10.1016/j.biocon.2012.01.018.

Holm, S., 1979. A simple sequentially rejective multiple test procedure. Scand. J. Stat. 6, 65–70.

Johansson, V., Kindvall, O., Askling, J., Franzén, M., 2020. Extreme weather affects colonization–extinction dynamics and the persistence of a threatened butterfly. J. Appl. Ecol. 57, 1068–1077. https://doi.org/10.1111/1365-2664.13611.

Johnston, A., Fink, D., Reynolds, M.D., Hochachka, W.M., Sullivan, B.L., Bruns, N.E., Hallstein, E., Merrifield, M.S., Matsumoto, S., Kelling, S., 2015. Abundance models improve spatial and temporal prioritization of conservation resources. Ecol. Appl. 25, 1749–1756. https://doi.org/10.1890/14-1826.1.

Jovani, R., Mavor, R., Oro, D., 2008. Hidden patterns of colony size variation in seabirds: a logarithmic point of view. Oikos 117, 1774–1781. https://doi.org/10.1111/j.1600-0706.2008.17065.x.

Kéry, M., Royle, J.A., 2016. Applied Hierarchical Modeling in Ecology: Analysis of Distribution, Abundance and Species Richness in R and BUGS, 1. Academic Press, London.

Kukkala, A.S., Moilanen, A., 2013. Core concepts of spatial prioritisation in systematic conservation planning. Biol. Rev. 88, 443–464. https://doi.org/10.1111/brv.12008.

Margules, C.R., Pressey, R.L., 2000. Systematic conservation planning. Nature 405, 243–253. https://doi.org/10.1038/35012251.

Maron, M., Hobbs, R.J., Moilanen, A., Matthews, J.W., Christie, K., Gardner, T.A., Keith, D.A., Lindenmayer, D.B., McAlpine, C.A., 2012. Faustian bargains? Restoration realities in the context of biodiversity offset policies. Biol. Conserv. 155, 141–148. https://doi.org/10.1016/j.biocon.2012.06.003.

McLaughlin, J.F., Hellmann, J.J., Boggs, C.L., Ehrlich, P.R., 2002. Climate change hastens population extinctions. Proc. Natl. Acad. Sci. USA 99, 6070–6074. https://doi.org/10.1073/pnas.052131199.

Nowicki, P., Halecki, W., Kalarus, K., 2013. All natural habitat edges matter equally for endangered *Maculinea* butterflies. J. Insect Conserv. 17, 139–146. https://doi.org/10.1007/s10841-012-9492-1.

Pech, P., Konvička, M., Spitzer, L., 2026. Vast alluvial meadows fail to provide habitats to host ants of the butterfly *Phengaris nausithous* along upper Oder river. J. Insect Conserv. 30, 19. https://doi.org/10.1007/s10841-026-00754-3.

Petitgas, P., 1998. Biomass-dependent dynamics of fish spatial distributions characterized by geostatistical aggregation curves. ICES J. Mar. Sci. 55, 443–453. https://doi.org/10.1006/jmsc.1997.0345.

Pulliam, H.R., 1988. Sources, sinks, and population regulation. Am. Nat. 132, 652–661.

R Core Team, 2025. R: A Language and Environment for Statistical Computing. R Foundation for Statistical Computing, Vienna, Austria. https://www.R-project.org/.

Sadovy, Y., Domeier, M., 2005. Are aggregation-fisheries sustainable? Reef fish fisheries as a case study. Coral Reefs 24, 254–262. https://doi.org/10.1007/s00338-005-0474-6.

Schtickzelle, N., Choutt, J., Goffart, P., Fichefet, V., Baguette, M., 2005. Metapopulation dynamics and conservation of the marsh fritillary butterfly: population viability analysis and management options for a critically endangered species in Western Europe. Biol. Conserv. 126, 569–581.

Slatyer, R.A., Hirst, M., Sexton, J.P., 2013. Niche breadth predicts geographical range size: a general ecological pattern. Ecol. Lett. 16, 1104–1114. https://doi.org/10.1111/ele.12140.

Swedish Environmental Protection Agency, 2020. Nationella Marktäckedata (NMD). Swedish Environmental Protection Agency, Stockholm. https://www.naturvardsverket.se/nmd. (Accessed 10 October 2024).

Swedish Environmental Protection Agency, 2022. Markfuktighetsindex, Nationella marktäckedata (NMD). Swedish Environmental Protection Agency, Stockholm. https://www.naturvardsverket.se/nmd. (Accessed 15 November 2024).

Taylor, L.R., 1961. Aggregation, variance and the mean. Nature 189, 732–735. https://doi.org/10.1038/189732a0.

Thomas, J.A., Simcox, D.J., Clarke, R.T., 2009. Successful conservation of a threatened *Maculinea* butterfly. Science 325, 80–83. https://doi.org/10.1126/science.1175726.

Thomas, J.A., Meredith, S.A., Simcox, D.J., 2025. Densities of the endangered large blue butterfly Phengaris arion vary by 100-fold in restored conservation grasslands, providing a tool to prioritise future introductions. J. Appl. Ecol. 62, 1463–1472. https://doi.org/10.1111/1365-2664.70065.

Todisco, V., Gratton, P., Cesaroni, D., Sbordoni, V., 2010. Phylogeography of *Parnassius apollo*: hints on taxonomy and conservation of a vulnerable glacial butterfly invader. Biol. J. Linn. Soc. 101, 169–183. https://doi.org/10.1111/j.1095-8312.2010.01476.x.

van Swaay, C.A.M., Schmucki, R., Roy, D.B., Dennis, E.B., Collins, S., Fox, R., et al., 2026. EU Grassland Butterfly Index 1991–2024 Technical Report. Butterfly Conservation Europe, EMBRACE/eBMS and De Vlinderstichting, Wageningen. Report VS2025.023.

WallisDeVries, M.F., van Swaay, C.A.M., 2006. Global warming and excess nitrogen may induce butterfly decline by microclimatic cooling. Glob. Chang. Biol. 12, 1620–1626. https://doi.org/10.1111/j.1365-2486.2006.01202.x.

Warren, M.S., 1994. The UK status and suspected metapopulation structure of a threatened European butterfly, the marsh fritillary Eurodryas aurinia. Biol. Conserv. 67, 239–249.

Warren, M.S., Maes, D., van Swaay, C.A.M., Goffart, P., Van Dyck, H., Bourn, N.A.D., Wynhoff, I., Hoare, D., Ellis, S., 2021. The decline of butterflies in Europe: problems, significance, and possible solutions. Proc. Natl. Acad. Sci. USA 118, e2002551117. https://doi.org/10.1073/pnas.2002551117.

Weiner, J., Solbrig, O.T., 1984. The meaning and measurement of size hierarchies in plant populations. Oecologia 61, 334–336. https://doi.org/10.1007/BF00379630.

Wittebolle, L., Marzorati, M., Clement, L., Balloi, A., Daffonchio, D., Heylen, K., De Vos, P., Verstraete, W., Boon, N., 2009. Initial community evenness favours functionality under selective stress. Nature 458, 623–626. https://doi.org/10.1038/nature07840.

Woillez, M., Poulard, J.-C., Rivoirard, J., Petitgas, P., Bez, N., 2007. Indices for capturing spatial patterns and their evolution in time, with application to European hake (Merluccius merluccius) in the Bay of Biscay. ICES J. Mar. Sci. 64, 537–550. https://doi.org/10.1093/icesjms/fsm025.

Wood, S.N., 2017. Generalized Additive Models: An Introduction with R, second ed. Chapman and Hall/CRC, Boca Raton, FL.

Zuur, A.F., Ieno, E.N., Walker, N.J., Saveliev, A.A., Smith, G.M., 2009. Mixed Effects Models and Extensions in Ecology with R. Springer, New York.